RESEARCH ARTICLE

Neuronal processing of translational optic flow in the visual system of the shore crab *Carcinus maenas*

B. Geoff Horseman[1,2], Martin W. S. Macauley[3] and W. Jon P. Barnes[1,*]

[1]Institute of Molecular, Cell and Systems Biology, University of Glasgow, Glasgow G12 8QQ, UK, [2]Cambridge Electronic Design, Unit 4, The Science Park, Milton Road, Cambridge CB4 0FE, UK and [3]School of Engineering, University of Glasgow, Glasgow G12 8QQ, UK

*Author for correspondence (Jon.Barnes@glasgow.ac.uk)

SUMMARY

This paper describes a search for neurones sensitive to optic flow in the visual system of the shore crab *Carcinus maenas* using a procedure developed from that of Krapp and Hengstenberg. This involved determining local motion sensitivity and its directional selectivity at many points within the neurone's receptive field and plotting the results on a map. Our results showed that local preferred directions of motion are independent of velocity, stimulus shape and type of motion (circular or linear). Global response maps thus clearly represent real properties of the neurones' receptive fields. Using this method, we have discovered two families of interneurones sensitive to translational optic flow. The first family has its terminal arborisations in the lobula of the optic lobe, the second family in the medulla. The response maps of the lobula neurones (which appear to be monostratified lobular giant neurones) show a clear focus of expansion centred on or just above the horizon, but at significantly different azimuth angles. Response maps such as these, consisting of patterns of movement vectors radiating from a pole, would be expected of neurones responding to self-motion in a particular direction. They would be stimulated when the crab moves towards the pole of the neurone's receptive field. The response maps of the medulla neurones show a focus of contraction, approximately centred on the horizon, but at significantly different azimuth angles. Such neurones would be stimulated when the crab walked away from the pole of the neurone's receptive field. We hypothesise that both the lobula and the medulla interneurones are representatives of arrays of cells, each of which would be optimally activated by self-motion in a different direction. The lobula neurones would be stimulated by the approaching scene and the medulla neurones by the receding scene. Neurones tuned to translational optic flow provide information on the three-dimensional layout of the environment and are thought to play a role in the judgment of heading.

Key words: Crustacea, crab, optic flow, self-motion detection, visual interneurone.

INTRODUCTION

Vision plays a key role in the majority of animals for their survival. However, the variety of eye types and the functions for which they are adapted is huge (Land and Nilsson, 2002). In contrast to the camera eyes of vertebrates, many arthropods have compound eyes, made up of individual units called ommatidia, each of which has its own lens system and photoreceptors. Such compound eyes have two major subtypes, apposition and superposition, that are adapted for vision under high and low light intensities, respectively (Land, 1981). The eyes of crabs are known as parabolic superposition eyes (there are also reflecting and refracting superposition eye types), and each ommatidium uses a mixture of lens and mirror optics to form an image of a small part of the field of view at the tip of the rhabdom, the part of the eye where the visual pigment is located (Nilsson, 1988). Compared with humans, both spatial acuity and colour vision are poor, but the eyes do detect ultraviolet light and are sensitive to the plane of polarisation of light. The latter ability is particularly useful for seeing reflecting surfaces (Zeil and Zanker, 1997) and, at least in insects such as bees, is used for navigation. Crab eyes, though lacking a fovea, have a band of high acuity located around the equator of the eye, which is particularly pronounced in 'flat-world' crabs that live on sand or mud flats, though less so in 'complex-environment' crabs such as the shore crab *Carcinus* (Zeil et al., 1986; Zeil et al., 1989), the crab used in this study.

As well as the perception of brightness and colour, eyes detect form and movement, and this motion perception is involved in a multitude of behavioural tasks including finding and/or selecting a mate, avoiding predators and catching prey, as well as more basic tasks such as control of balance and those that contribute to oculomotor reflexes. Motion detection can also be used by animals to detect their own movements (self-motion) in order to navigate through its surroundings. Therefore, the detection of movement plays a very important part in an animal's life and, consequently, has been an active field of research (for reviews, see Land, 1999; Eckert and Zeil, 2001).

Of particular interest is the image motion over the retina of the eye resulting from an animal moving through its surroundings, first described by Gibson over 60 years ago (Gibson, 1950). The term 'optic flow' was used by Gibson to describe these images and his studies were aimed at understanding the role of optic flow in visual perception and guidance (Gibson, 1950; Gibson, 1966; Gibson, 1986). The mathematics underlying these studies was described by Koenderink and Van Doorn (Koenderink and Van Doorn, 1987) and has led to rapid advances in computer vision and the

development of autonomous robots that can navigate on the basis of optic flow (e.g. Srinivasan et al., 1999; Green et al., 2004; Hyslop et al., 2010). Optic flow can be split into two components, rotational and translational. Active turning results in a rotational optic flow field in which all the vectors (indicating direction of motion and its velocity) at a given elevation have the same length, irrespective of the distance of the objects in the image, and they all point in the opposite direction to the movement. Motion in a straight line, however, produces a translational flow field with a pole or focus of expansion in the direction of travel, and vector length depends on both the angle of the contour relative to the direction of travel and the distance of objects from the eye. Gibson demonstrated that the rotational component could be used to correct deviations from an intended path whereas the translational component provides animals with a large amount of information about their own movement, such as velocity, distance covered and heading (Gibson, 1966). Since this time, evidence has accumulated for the involvement of optic flow in tasks such as distance estimation (David, 1982; Srinivasan et al., 1991), collision avoidance (Holmqvist and Srinivasan, 1991; Tammero and Dickinson, 2002), maintenance of a constant heading (Collett and Land, 1975), course stabilization and oculomotor control (Hassenstein and Reichardt, 1956; Götz, 1975), triggering of landing responses (Wagner, 1982) and control of moth–flower distance in hovering flight (Farina et al., 1994).

Within the vertebrates, optic flow neurones have been recorded from both birds and mammals, including the mammalian vestibulocerebellum (Simpson et al., 1981), primate dorsal medial superior temporal area (Saito et al., 1986; Tanaka and Saito, 1989; Paolini et al., 2000), primate ventral intraparietal area (Bremmer et al., 2002) and avian nucleus rotundus (Wang and Frost, 1992; Wylie and Frost, 1993; Sun and Frost, 1998). Optic flow neurones of insects include neurones in hovering moths that respond to looming or receding stimuli (Wicklein and Strausfeld, 2000), but undoubtedly the best understood system is the lobula plate (third optic neuropil) of blowflies. This contains approximately 60 wide-field directionally selective visual interneurones called tangential neurones (Hausen, 1982a; Hausen, 1982b; Hausen, 1984; Hausen and Egelhaaf, 1989). Elegant experiments by Krapp and Hengstenberg (Krapp and Hengstenberg, 1996) and Krapp et al. (Krapp et al., 1998) [reviewed by Krapp (Krapp, 2000) and extended by Haag and Borst (Haag and Borst, 2004) amongst others], have revealed that many of these neurones have distributions of local preferred directions (LPDs) and local motion sensitivities (LMSs) that show a striking similarity to those of optic flow fields. The findings suggest that each tangential neurone is tuned to process image flow generated by specific movements of the flying insect (for a review, see Taylor and Krapp, 2007).

Much less is known about the visual system of crustaceans. Early work identified response properties of interneurones of the optic nerve to simple stimuli. These included sustaining fibres, dimming fibres and several classes of motion detectors (Waterman et al., 1964; Wiersma, 1966; Wiersma and Yamaguchi, 1966; Wiersma and Yamaguchi, 1967; York and Wiersma, 1975) (reviewed in Wiersma et al., 1982). Subsequent studies based on intracellular recording and Lucifer Yellow injections confirmed the identity of many of the sustaining fibres (Kirk et al., 1982; Kirk et al., 1983). More recent work on the neural integration of motion stimuli of particular relevance to this study examined the properties of neurones responsive to looming stimuli that elicit escape (Tomsic et al., 2003; Medan et al., 2007; Oliva et al., 2007; Sztarker and Tomsic, 2008).

The present study examines the responses of visual neurones sensitive to optic flow in the visual system of the shore crab using Krapp and Hengstenberg's procedure (Krapp and Hengstenberg, 1997) adapted for crabs (Johnson et al., 2002) and other visual stimulation methods. This involves determining the local motion sensitivity at many points within the receptive field. The map of LPDs and LMSs derived in this way then reveals the cell's global motion sensitivity. Using this method, we discovered two families of interneurones sensitive to optic flow, one in the lobula and the other in the medulla. We hypothesise that the lobula and medulla interneurones are representatives of arrays of cells with poles at different azimuth angles, each of which would be optimally activated by self-motion in a different direction. The lobula neurones would be stimulated by the approaching scene, the medulla neurones by the receding scene. Preliminary accounts of these experiments appear in Barnes et al. (Barnes et al., 2001; Barnes et al., 2002).

MATERIALS AND METHODS
Animals
Experiments were performed on shore crabs *Carcinus maenas* (Linnaeus 1758) collected from the Firth of Clyde, Scotland (Millport Marine Station). They were maintained for up 2 months in holding tanks of circulating seawater (10°C, 12 h:12 h light:dark regime) before use. They were fed once a week on a diet of fish.

Preparation
Recordings were made from the right eyestalk of crabs of both sexes (carapace width=5–7 cm). Each crab was first induced to autotomise the chelae, and was mounted horizontally in a clamp. The right eyestalk was then fixed to the carapace with cyanoacrylate cement in a natural 'raised' position while the left eye was glued into a position fully withdrawn into its socket. In order to make intracellular recordings from visual interneurones in the optic lobe it was necessary to exchange the blood for oxygenated Ringer's solution. This was done by a method broadly similar to that described for crayfish (Kirk et al., 1982; Glantz and Bartels, 1994). The hypodermis dorsal to the heart was exposed by making a circular cut (*ca.* 1 cm in diameter) through the cardiac region of the carapace using a dental drill. The circular flap of cuticle thus formed was carefully removed without puncturing the skin. A similar area of hypodermis in the left protogastric region of the carapace [nomenclature of Pearson (Pearson, 1908)] was exposed in the same way. The crab was then lowered into a bath of cold (6°C) oxygenated *Carcinus* Ringer's solution (500 mmol l^{-1} NaCl, 12 mmol l^{-1} KCl, 12 mmol l^{-1} CaCl$_2$, 20 mmol l^{-1} MgCl$_2$, 10 mmol l^{-1} Tris, 2 mmol l^{-1} maleic acid, 2 mmol l^{-1} glucose; pH 7.3) [modified after Bush and Roberts (Bush and Roberts, 1971)]. The exposed hypodermis above the heart was then cut away, the pericardium was torn and the blood was allowed to exchange with the surrounding Ringer's solution. This process was accelerated by injecting Ringer's solution into the main chamber of the heart (10–15 ml min^{-1}) *via* a syringe and hypodermic needle.

After 25 min of exsanguination, the crab was connected to a gravity-fed system to perfuse the circulatory system continuously with oxygenated Ringer's solution. The crab was first raised above the surface of the Ringer's solution. Then a cannula was introduced into the hole in the carapace above the heart and sealed in position with a combination of cyanoacrylate cement and Blu Tack^{TM} (Bostik, Wauwatosa, WI, USA). The flow rate was set to ~3 ml min^{-1}. The previously exposed hypodermis in the protogastric region was cut away and the underlying blood sinuses were opened to provide a route for the outflow of Ringer's solution. In some preparations it was necessary to displace the exposed part of the stomach posteriorly and glue it to the carapace to prevent it from

ballooning out through the hole and blocking the outflow of Ringer's solution. After re-immersing the crab, the right optic lobe was exposed by whittling away the overlying eyestalk cuticle with a scalpel blade, removing the hypodermis and desheathing the optic ganglia in the region of interest. The crab was removed from the saline bath and transferred to the experimental setup.

Visual stimulation

Visual stimuli were back-projected onto two flat screens (38×32 cm) that formed two sides of an equilateral triangle (Fig. 1). The crab was positioned midway between the two screens, facing the apex, with the right eye at the midpoint of the triangle. In this way, images could be projected over an angular range relative to the eye of 240 deg in azimuth (0 to 120 deg on the right screen, 0 to –120 deg on the left) and ~100 deg in elevation (typically –40 to +60 deg relative to the crab's horizon).

The test stimuli were generated by computer programs written in the Turbo Pascal or Borland Delphi languages, and running on PCs. They were projected *via* angled plane mirrors onto each screen with LCD computer projectors (Panasonic PT-L291EG, resolution 640×480 pixels, contrast ratio 150:1; Panasonic Corp., Osaka, Japan). Using a light meter placed at the position normally occupied by the crab, we measured maximum (I_{max}) and minimum (I_{min}) luminance of our stimuli (using a 'completely white' and 'completely dark' screen, respectively) of 42.2 and 0.33 cd m^{-2}, respectively. The Michelson contrast [$(I_{max}-I_{min})/(I_{max}+I_{min})$] was therefore 0.98. The main stimuli used in this study were: a moving white disc (Fig. 2B), a flashing white disc (Fig. 2C), small-field straight line motion (Fig. 2D), small-field circular motion (Fig. 2E) and small-field circular motion compensated for distortions due to perspective (Fig. 2F), as described previously (Johnson et al., 2002). Responses to local motion stimuli were tested at fixed angular intervals, typically of 15 deg azimuth and elevation at the intersections of the grid shown in Fig. 2A.

As Barnes et al. (Barnes et al., 2002) have shown, our computer-generated stimuli are entirely suitable for crab visual system research. In particular, the refresh rate of our computer projectors, 70 Hz, was significantly higher than crab flicker fusion rates (50 Hz light-adapted and 32 Hz dark-adapted) measured in the fiddler crab, *Uca pugilator* (Layne et al., 1997). Secondly, the spatial resolution of our experimental setup (0.1875 deg pixel^{-1}) was over 10 times greater than the best spatial resolution of the *Carcinus* eye [2 deg (Zeil et al., 1986)].

Intracellular recording and staining

Intracellular recordings were made using either thin-walled (1 mm outer diameter, 0.22 mm wall, impedance 40 MΩ) or thick-walled (1 mm outer diameter, 0.42 mm wall, impedance 110 MΩ) borosilicate glass microelectrodes, filled with 4% Lucifer Yellow in the tip and 1 mol l^{-1} lithium chloride in the barrel. Neural responses and monitors of intracellular current injection and the visual stimulus were amplified conventionally and recorded online using a CED1401 Plus interface and Spike 2 (both Cambridge Electronic Design, Cambridge, UK) software running on a PC. Subsequent data analysis was performed using Spike 2 scripts. Raw data and analysed results were stored on the hard drive and recordable compact discs.

Neuronal morphology was investigated using Lucifer Yellow dye injection (Stewart, 1978). Cells were dye-filled using approximately –4 nA continuous current injection for as long as possible. In practice, this varied from 5 to 90 min. As soon as the recording was over, a drop of fixative was applied to the eyestalk to initiate the fixation
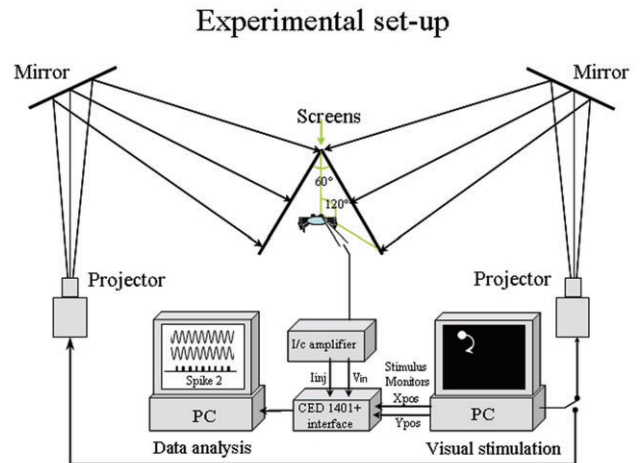

Fig. 1. The setup for visual stimulation and intracellular recording. For simplicity, one computer is shown as controlling the visual stimulus either on the right or the left screen *via* a switch. In practice, two computers were used, one controlling each projector (see Materials and methods for further details). I/c amplifier, intracellular amplifier; I_{inj}, current injection monitor; V_{in}, intracellular recorded membrane potential; x_{pos}, y_{pos}, x- and y-coordinates of visual stimulus, respectively.

process. Then the whole eyestalk was removed from the crab and dissected in fixative. The fixative consisted of 3.7% formaldehyde with added sucrose (15 g per 100 ml) in a phosphate buffer (5 g NaCl, 14 g Na$_2$HPO$_4$·2H$_2$O and 3.2 g NaH$_2$PO$_4$·2H$_2$O, dissolved in 1 l of distilled water). Both fixative and buffer were adjusted to pH 7.3 with 1 mol l^{-1} NaOH. It was found that the fixative did not penetrate properly unless the optic ganglia were dissected out of the eyestalk. Preparations were then left to fixate overnight in a refrigerator. Reconstructions of neuronal morphology were carried out on whole mounts viewed under a fluorescence microscope.

Data analysis

Some pre-treatment of the data was necessary, e.g. using Spike 2 peak detection or threshold facilities to generate an event channel for nerve impulses based on the waveform of an intracellular recording. However, after this the analysis was semi-automatic. Examples of the stages involved in deriving the directional motion sensitivity of a neurone to small-field circular motion at an individual screen locus (Krapp and Hengstenberg, 1997) are shown in Fig. 3. The first stage was to generate a phase diagram of the response to anticlockwise motion (Fig. 3A), based either on impulse activity or a signal mean of non-spiking responses (Fig. 3C). The mean preferred direction was derived by circular statistics (Batschelet, 1981). A similar phase diagram of the response to clockwise rotation (Fig. 3D) is not directly comparable because the sequence of motion directions tested is different. However, the clockwise plot can be made comparable to the anticlockwise response by reversing it (i.e. rotating it about its *x*-axis) and then phase-shifting it by 180 deg (Fig. 3E). Clearly, the curves for anticlockwise and clockwise motion still do not match. This is because the anticlockwise distribution is subject to an unknown phase lag whereas in the clockwise distribution, this has been converted to an equal phase lead because of the flip and shift transformation of the data. Thus, the two distributions are separated by two times the phase shift. The true preferred direction is derived by shifting the anticlockwise distribution clockwise (to eliminate phase lag), and the clockwise
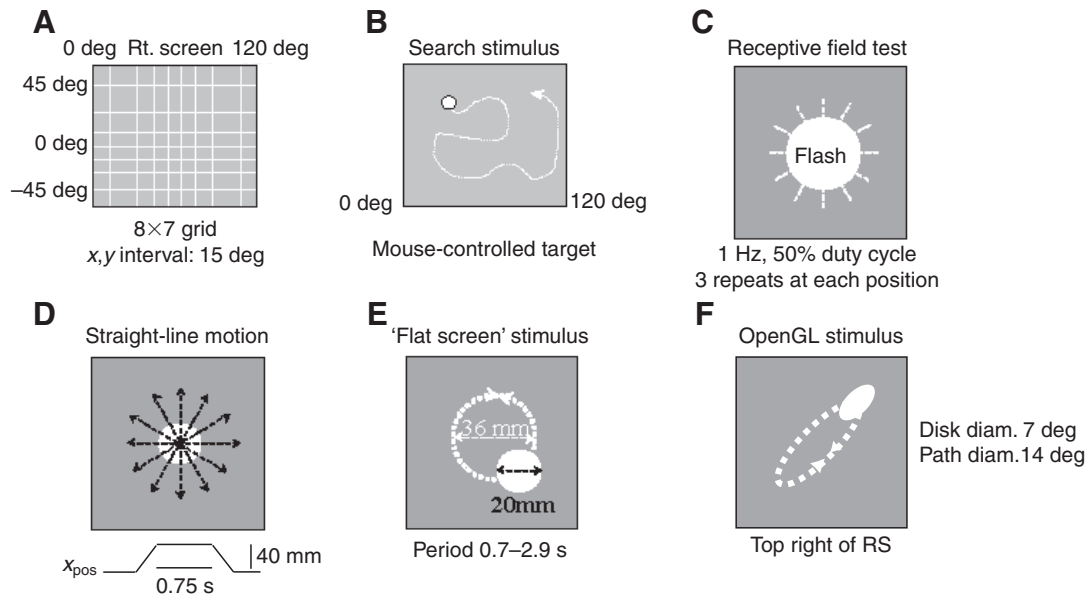
A

0 deg Rt. screen 120 deg

45 deg

0 deg

−45 deg

8×7 grid
x,y interval: 15 deg

B

Search stimulus

0 deg   120 deg

Mouse-controlled target

C

Receptive field test

Flash

1 Hz, 50% duty cycle
3 repeats at each position

D

Straight-line motion

x_{pos} ___ 40 mm
0.75 s

E

'Flat screen' stimulus

36 mm

20mm

Period 0.7–2.9 s

F

OpenGL stimulus

Disk diam. 7 deg
Path diam.14 deg

Top right of RS

Fig. 2. (A) Diagram showing the angular coverage of one screen. Intersections on the 8×7 grid mark the standardised screen coordinates at which local motion stimuli were presented. (B–F) Images of the most commonly used local stimuli. (B) The stimulus used to search for motion-sensitive neurones and estimate their receptive fields was a white disc (diameter 30 mm) moved over a black background using the computer mouse. (C) Receptive fields were further characterised from responses to a flashing white disc (diameter 30 mm) at each test locus. (D) Responses to linear motion at a range of angles were tested with a white disc (diameter 22 mm) or bar (38×9 mm) moving to and fro. The monitor trace indicates stimulus amplitude and timing. (E) The 'flat-screen' rotating stimulus was a white disc (diameter 20 mm) moving at constant angular velocity in a circle of diameter 36 mm. In each trial, the disc rotated anticlockwise and then clockwise for an equal number of cycles. The stimulus was then moved to another part of the screen. Because the eye was closer to the centre than to the edges of the screen, the angle subtended at the eye by stimuli B–E depended upon screen location. Mean values of this angle were (B,C) 10 deg, (D) 7.4 or 12.4 deg × 4 deg and (E) 6.6 deg in a circle of 12 deg. (F) In later experiments we used a rotation program that predistorted the image so that, from the crab's viewpoint, the path and shape of the target remained circular and the angular velocity appeared constant despite the effects of perspective. From the viewpoint of the experimenter, the target and its path appeared elliptical near the edges of the screen.

distribution anticlockwise (to eliminate phase lead), until the mean vectors are aligned. The true mean vector is obtained by averaging the two distributions and recalculating the circular statistics (Fig. 3F). During the analysis, a provisional response map is built up progressively as each response at a new screen position is analysed on a Mercator map of visual space. A vector is drawn at each position tested, the angle indicating the local preferred direction of motion. The vector length is *r*, indicating the local strength of this direction preference; *r*=1 means that all events fall within the same directional bin whereas *r*=0 means that they are equally distributed over the full 360 deg angular range. Once all the data are analysed, an LMS response map can be generated. Here, local motion sensitivity is defined as mean response in a 90 deg sector that is centred on the LPD minus the response in the 90 deg sector centred on the opposite direction. Vector lengths can be normalised relative to the largest to generate a map that facilitates comparison of sensitivity patterns between individuals.

A second method of generating the polar plots from which the LPDs and LMSs are calculated used straight-line motion (Fig. 4). In these linear motion tests, the same target disc moved, at constant speed, back and forth across the diameter of the circular path followed in the rotating disc paradigm (Fig. 4A). The target remained stationary for a fixed time at the end of each sweep so that the unknown response latency did not lead to ambiguity between responses to motion in opposite directions (Fig. 4B). After a fixed number of sweeps, the 'diameter' tested was advanced by 30 deg and the process repeated until all 12 directions had been tested. The initial pair of directions was then repeated as a control for adaptation of motion sensitivity during the sequence. Polar directional plots were based on accumulated spike counts for each motion direction (Fig. 4C), and the LPD was derived from this using circular statistics (Batschelet, 1981). In practice, this method was generally applied at relatively few screen loci in order to corroborate the analysis based on rotational motion. This was because the linear motion stimulus was more time consuming and has a much lower resolution.

RESULTS

Our analysis of the properties of wide-field motion-detecting neurones that might be involved in the detection of optic flow involved a two-stage process. First, the direction of local motion sensitivity was analysed at many different points within the neurone's receptive field. Then the resulting vectors, representing the direction and strength of motion sensitivity at each analysed position, were used to compile a map of the cell's global motion sensitivity.

Analysing local motion sensitivity in wide-field visual interneurones

The initial stimulus used to search for motion-sensitive neurones and estimate their receptive fields was a white disc moved over a black background using the computer mouse (Fig. 2B). Receptive fields were further characterised from responses to a flashing white disc at each test locus (Fig. 2C). Only motion-sensitive neurones with large receptive fields (>90 deg of arc) were studied further. Neurones with the above properties were found in both the medulla and lobula neuropils of the optic tract [terminology of Sztarker et al. (Sztarker et al., 2005)].
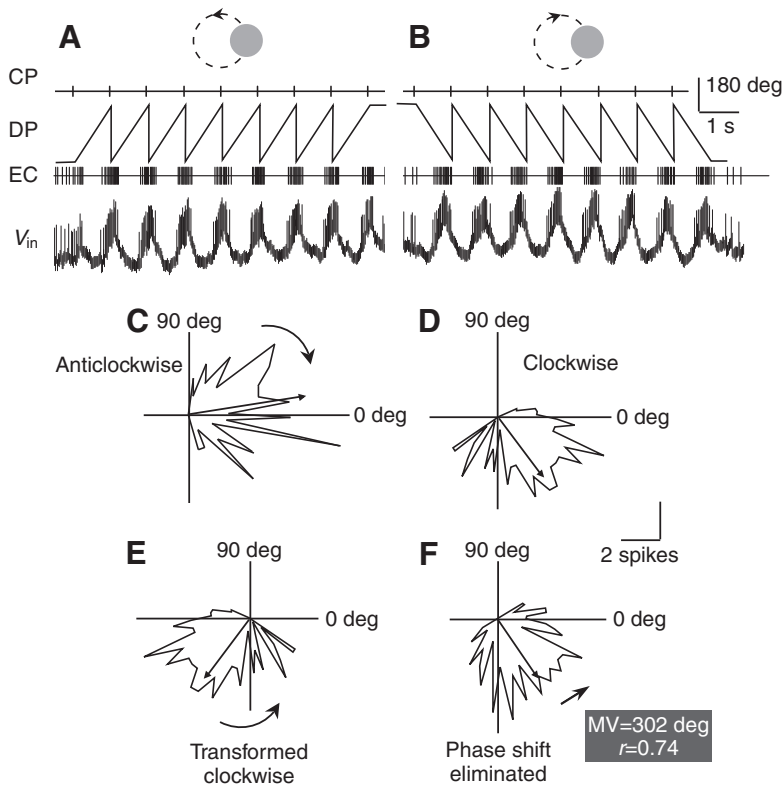
Fig. 3. Using a rotating disc to determine local motion selectivity. (A,B) Example responses recorded from a *Carcinus maenas* interneurone with its dendritic arborisation in the medulla of the right optic lobe to eight cycles of (A) anticlockwise and (B) clockwise movement of the predistorted rotating disc stimulus (see Fig. 2F). CP, cycle period; DP, disc position; EC, event channel showing timing of nerve impulses recorded in the intracellular recorded membrane potential (V_{in}). (C,D) Phase diagrams of the accumulated response to anticlockwise and clockwise motion over eight cycles in each direction. Each plot shows the mean vector (MV) and vector length *r* (arrows) (*r* is a measure of concentration about the mean direction) (Batschelet, 1981). (E) The response to clockwise motion is reversed and phase shifted by 180 deg, the transformation required to make the sequence of motion directions the same as that in the phase plot for anticlockwise motion. Clearly, the response curves for anticlockwise and clockwise motion still do not match. This is because the response to anticlockwise motion includes a phase lag due to the latency and temporal filtering characteristics of the visual system, whereas the clockwise data is phase advanced by the same amount due to the transformation shown in E. (F) The local preferred direction of motion (LPD) is derived by rotating the anticlockwise and clockwise distributions in the direction shown by the curved arrows in C and E until the mean vectors are aligned. This mean vector points to the position in an anticlockwise cycle at which the neurone responded maximally. The direction of motion at that position is phase advanced by 90 deg (arrow). The bin size for plots C–F is 5 deg.

LPDs of motion sensitivity were analysed from the responses to the rotation of a white disc moved in a circle, first anticlockwise for a number of cycles and then clockwise for the same number of cycles (Fig. 2E,F). As Fig. 3 illustrates, most of these neurones responded with bursts of nerve impulses to these local stimuli whenever the movement was in the preferred direction for this location within the receptive field, though we have also analysed subthreshold responses (data not shown). Polar phase diagrams were separately compiled for clockwise and anticlockwise responses (Fig. 3C,D) and then, after appropriate transformations (see figure legend and Fig. 3E), combined to give the final polar plot (Fig. 3F).

LPDs were also calculated from responses to straight-line motion rather than rotation (Fig. 2D). Fig. 4 shows a typical example of the responses obtained from a neurone in the medulla. The response is phasotonic, the firing frequency remaining high for a period after the end of the movement (Fig. 4B). Note that movement in the opposite direction produces inhibition. Exactly the same screen positions could be tested with the two different methods to provide a check of the directional selectivity. Polar directional plots (e.g. Fig. 4C) were based on accumulated spike counts for each motion direction. Resulting LPDs usually had smaller concentration parameter values than when circular motion stimuli were used (see below).

An example of such a check of directional selectivity appears in Fig. 5. It shows that LPDs are reassuringly robust and relatively insensitive to changes in speed of movement. Estimates of LPD for a single point in the neurone's receptive field are hardly affected by changing the velocity at which the disc is rotated for cycle periods between 0.5 and 3 s (Fig. 5A), though there is a halving of the value of the concentration parameter *r* for a fourfold increase in cycle period. These periods translate into angular velocities covering the range 35–200 deg s^{-1}. LPDs are also unaffected by the method used to compile them. When linear motion stimuli are used instead of a rotating disc (Fig. 5B–D shows three different points in the visual

field), the LPDs remain closely matched, though again the value of *r* is affected; it is lower for straight-line stimuli. The reduction in *r* for straight-line movements is, however, mostly a property of the way in which the polar plot was compiled for such movements, for they include the tonic as well as the phasic response to the movement (Fig. 4C). In Fig. 5E, we looked at one point in space, and used circular motion to assess the mean vector (plotted on the *y*-axis of the graph). This is affected by neither the period of the motion (*x*-axis of graph) nor the shape of the object moved, whether it be a spot, bar, annulus or lattice. The line of best fit is not significantly different from the horizontal (*t*-test, *P*>0.10). Together, these three tests make us confident that LPDs represent real properties of the neurones' receptive fields, rather than artifacts of the experimental method.

Response map compilation

Fig. 6A–D shows recordings from a wide-field motion-detecting neurone with its dendritic arborization in the medulla, and phase plots resulting from stimulating positions in space 20 deg apart in azimuth. There is a clear reversal of directional selectivity between the two points (mean ± s.d. phase shift=170±34 deg, *N*=47). Such a result makes it clear that we are dealing with a neurone with a complex receptive field. Local motion sensitivity was therefore analysed over the whole receptive field of the neurone, at all 56 standardised grid coordinates, and the resulting LPDs were then plotted onto a Mercator projection map of visual space. This map is shown in Fig. 6E (green vectors). It has a clear focus of contraction (FOC) at ~45 deg to the right of the midline at an elevation of approximately –20 deg (horizon=0 deg) and all vectors are directed approximately towards this point. The illustrated polar plots are situated on either side of the FOC in columns three and five of row four (asterisks). As a test of whether response maps depended on the type of visual stimulus, we used three different methods to calculate the LPDs in Fig. 6E: flat-screen rotational stimuli (Fig. 2E),
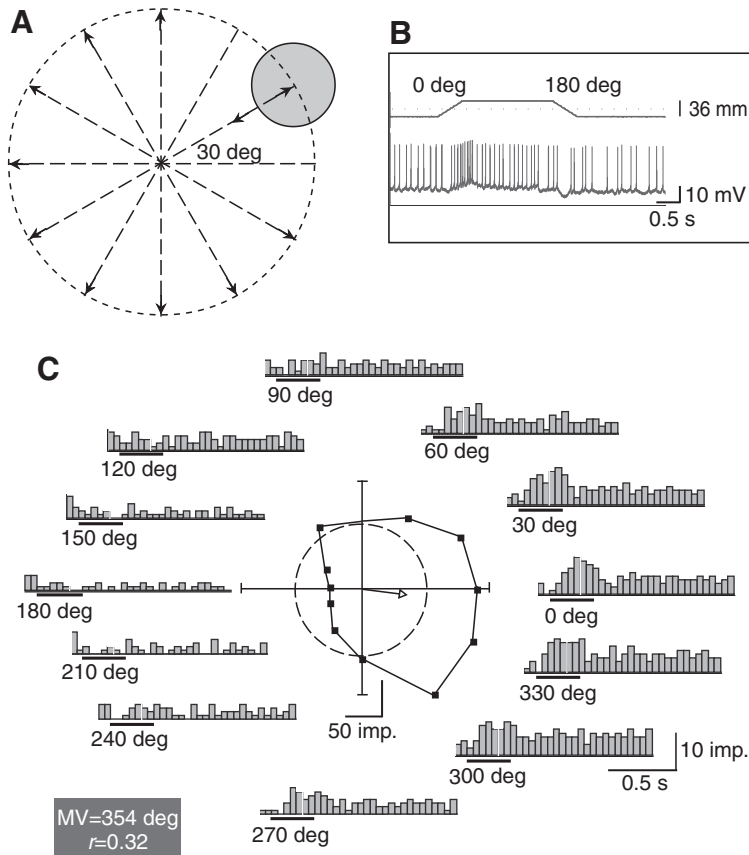
Fig. 4. Using straight-line motion to determine local motion selectivity (A) A white disc is moved at constant velocity back and forth across the diameter of a circle, each movement followed by a pause (see Fig. 2D). Four sweeps at 12 different orientations, 30 deg apart, were carried out at selected points in the cell's receptive fields. (B) Example response recorded from a *C. maenas* interneurone with its dendritic arborisation in the medulla of the right optic lobe (lower trace) to a sweep of straight-line motion at 0 deg followed by a sweep at 180 deg (upper trace). (C) Accumulated spike counts for each motion direction (histograms) were used to compile the polar plots, whereas the LPD (arrow) was derived from this by circular statistics (Batschelet, 1981). The line underneath each histogram indicates the time and duration of the disc movement. imp., nerve impulses; MV, mean vector; r=vector length, the value of the concentration parameter.

pre-distorted rotational stimuli (Fig. 2F) and straight-line motion (Fig. 2D). The response maps resulting from these different procedures are coloured green, black and red, respectively in Fig. 6E. Clearly there is a good match between the results obtained using the three different methods, an indication that such maps truly represent the cell's global motion sensitivity.

Variability of responses within crabs was tested on a number of occasions by repeating the compilation of the map of local motion sensitivity after an interval of approximately 30 min with the microelectrode still within the neurone. Consistent values were invariably obtained (data not shown).

Types of response map and their properties

Of the 18 preparations (out of a total of 27) where we have good data and have been able to compile response maps from up to three wide-field motion-sensitive neurones per preparation, we have successful Lucifer Yellow fills from 13 neurones. The majority of these have their dendritic arborisations in the lobula and their somata ventrally located between the lobula and the lateral protocerebrum. A smaller percentage has their dendritic arborisations in the medulla and their somata at the edge of the lobula near the sinus gland. All neurones anatomically identified as medulla neurones (Fig. 7A) had response maps characterised by an FOC (Fig. 7B) whereas all neurones anatomically identified as lobula neurones (Fig. 7C,E) had response maps characterised by a focus of expansion (FOE) (Fig. 7D,F). We conclude that we recorded from two arrays of neurones with opposite properties. Neurones receiving their inputs in the medulla have receptive fields characterised by an FOC and so would be stimulated by receding objects, whereas neurones receiving their inputs in the lobula have receptive fields characterized by an FOE and so would be stimulated by approaching objects.

Surprisingly, in view of the fact that high-gain optokinetic responses occur in crabs such as *Carcinus* (Horridge and Sandeman, 1964; Horridge, 1966; Barnes and Horridge, 1969), we did not record from neurones sensitive to rotational optic flow.

From experiments where we recorded from more than one neurone in a preparation (Fig. 8), it is clear that different neurones have poles at different azimuths. As far as medulla neurones are concerned, we recorded from cells where the azimuths of the FOCs were located 0 (frontal), 50–55, 90 and 120 deg to the right of frontal (N=10). For lobula neurones, the azimuths of the FOEs were located 30–40, 60–75 and 90–100 deg to the right of frontal (N=17). Presumably, the left optic lobe will include cells covering the area to the left of the midline. Examples of these are illustrated in Fig. 8. Whether the foci also have different elevations is less certain, because of possible errors (±10 deg) in the positioning of the eye. For medulla neurones, the range was –25 to +30 deg (horizon=0 deg) with a mean value of –5 deg (N=10), whereas for lobula neurones, the range was 0 to +48 deg with a mean of +22 deg (N=17). It certainly appears that the FOEs of lobula neurones are, in general, centred above the horizon.

The majority of response maps had a receptive field 90–120 deg in width and extending vertically from ~40 deg below to ~60 deg above the horizon (Fig. 7D and Fig. 8). A small minority were much wider in extent. For instance, the medulla neurone whose response map is shown in Fig. 7B extended from –65 to +65 deg, whereas the lobula neurone whose response map is illustrated in Fig. 7F extended from –115 to +115 deg. For all neurones where we both dye-filled the neurone and mapped its response field, there was a good correlation between the extent of the dendritic tree and the width of the response map (Fig. 7). Response maps of medulla neurones were relatively variable in shape. Fig. 8C shows a map where there is an
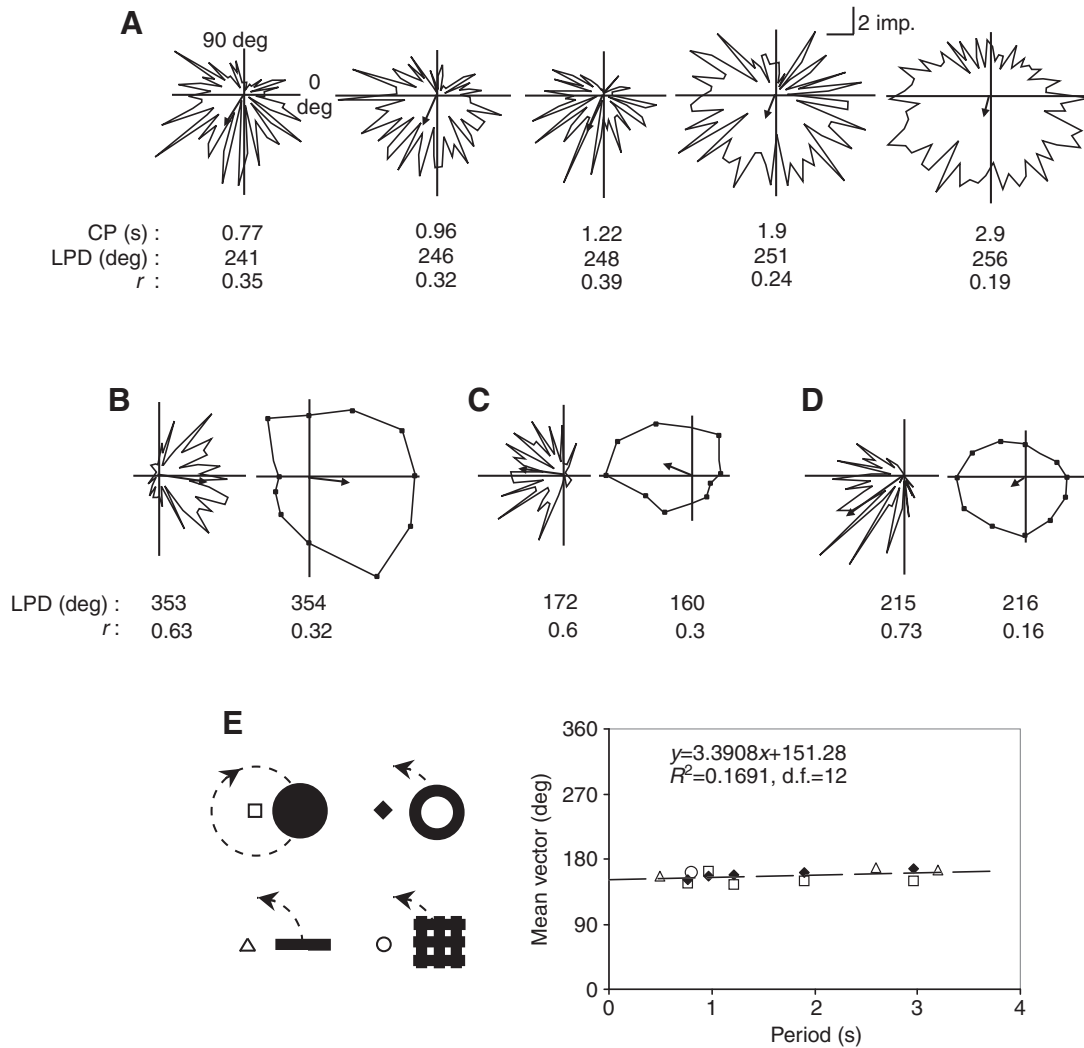
Fig. 5. Effect of stimulus type and period on LPDs. (A) Polar phase diagrams showing number of impulses fired in response to a disc rotating at various speeds (CP, cycle period), as a function of motion direction. The estimate of LPD is virtually independent of rotation speed within the range tested although the strength of the directionality (value of r) may vary. Data are from a *C. maenas* interneurone with its terminal arborisation in the medulla. (B–D) Comparison of LPD derived from rotation with that derived at the same screen position from linear motion stimuli (Fig. 2D) at three different screen locations. In each case, the phase plot for rotation is on the left and that for linear motion on the right. As in A, the phase plots for rotational stimuli have been advanced by 90 deg so that the vector indicates LPD directly. (E) Effect of CP (x-axis) and target shape on local preferred direction (y-axis). Target shapes tested were a white annulus (filled triangle), a disc (open square), a bar (open triangle) and a lattice pattern consisting of two horizontal and two vertical bars (open circle). The regression line on the graph has a slope that is not significantly different from zero (t-test).

extended vertical area around the FOC, whereas those in Fig. 7B and Fig. 8D show extended horizontal areas. A common feature of lobula neurone response maps, illustrated in Fig. 8A,B (but not in Fig. 7B), is for the response map to be extended horizontally, perhaps providing a template for the horizontal skylines that dominate most seascapes (Barnes et al., 2001; Eckert and Zeil, 2001).

Other properties of these neurones

The class of interneurone in which the dendritic arborisations occur in the medulla respond vigorously to the preferred direction of motion and are strongly inhibited by movements in the opposite direction (Fig. 6A,B). They also respond phasotonically to 'light on' and are momentarily hyperpolarised following 'light off' (Fig. 9A). Lobula neurones, however, showed 'on' and 'off' responses to a stationary light stimulus in addition to their response to movement (Fig. 9B). In a few experiments their distribution was mapped. Both 'on' and

'off' responses occurred in the central area of the receptive field, with 'off' responses extending towards the periphery of the receptive field more widely than 'on' responses (Fig. 8A).

DISCUSSION

Identity of the populations of medulla and lobula neurones with response maps characteristic of optic flow neurones

A number of different classes of visually responsive neurone, including sustaining fibres, dimming fibres and several different types of movement fibres, have been identified within the optic nerves of a variety of decapod crustaceans (for a review, see Wiersma et al., 1982). Each of these categories can be subdivided on the basis of the size and location of the neurone's excitatory receptive field, in some cases down to the level of individual physiologically identifiable neurones. Subsequent work on crayfish, based on intracellular recordings, has begun to give us insights into the neural circuitry of
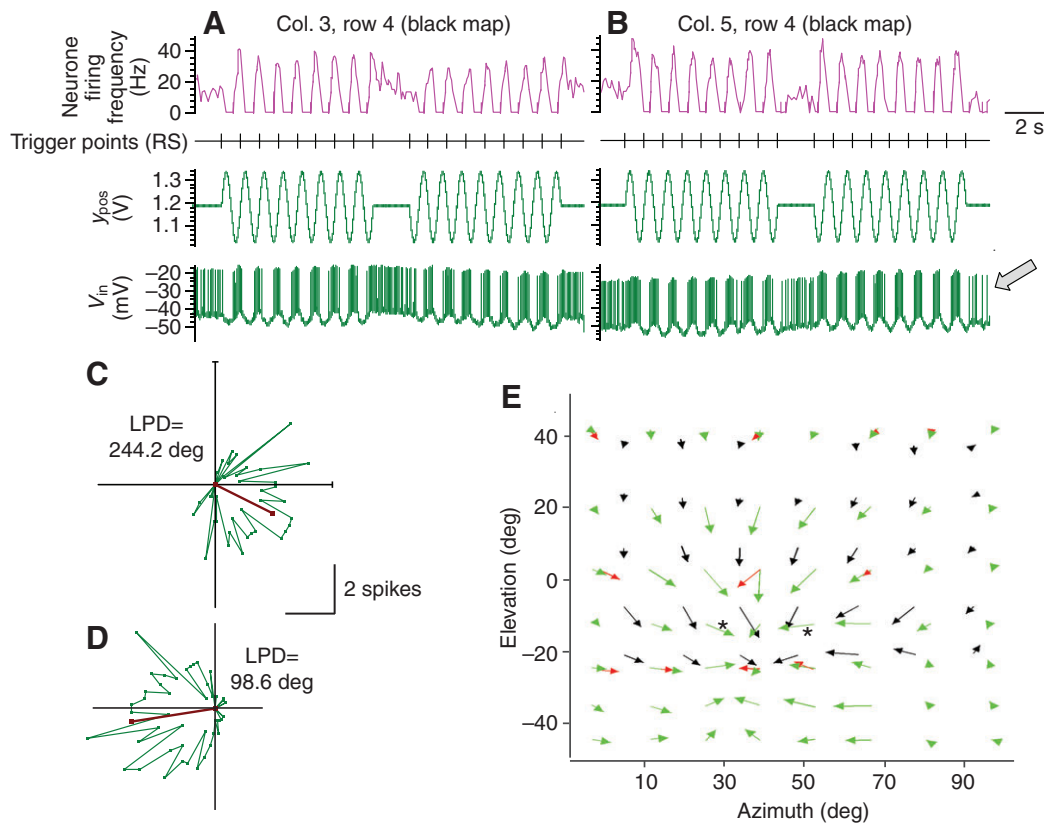
Fig. 6. (A,B) Responses recorded from a *C. maenas* interneurone with its dendritic arborisation in the medulla of the right optic lobe to eight cycles of anticlockwise and clockwise movement of the rotating disc stimulus (see Fig. 2E) at two points 20 deg apart in azimuth. Note the periods of inhibition following the bursts of spikes (arrow). (C,D) Polar plots of the combined response to anticlockwise and clockwise motion over eight cycles in each direction. Each plot shows the mean vector (red line) with vector length *r*, phase-shifted so that the vectors represent the LPDs. These two vectors are indicated by asterisks on the response map. (E) Response map. Arrows represent three sets of vectors showing the direction and strength of LPD: vectors derived from flat-screen rotational stimuli (green); those derived from pre-distorted rotational stimuli, i.e. of constant size and angular velocity irrespective of screen position (black); and those derived from straight-line motion (red). Note the clear focus of contraction (FOC) at ~45 deg to the right of frontal at an elevation of 25 deg below the horizon. RS, right screen; y_{pos}, *y*-axis position of disc; V_{in}, intracellular recorded membrane potential.

the optic tract (reviewed by Glantz and Miller, 2001). A more complete picture is emerging from recent work on the crab *Chasmagnathus*. This includes a thorough histological study based on silver staining of neurones (Sztarker et al., 2005; Sztarker et al., 2009) and a detailed analysis of the different properties of lobular neurones involved in escape responses to looming stimuli (Berón de Astrada and Tomsic, 2002; Medan et al., 2007; Oliva et al., 2007; Sztarker and Tomsic, 2008), several of which show a form of learning related to habituation (Tomsic et al., 2003). Yet none of this work refers to the term 'optic flow', nor have stimuli appropriate for the identification of neurones tuned to optic flow been used. It is clearly of interest to see how our work fits into this picture.

In crayfish, a class of visual interneurones known as sustaining fibres, initially called tonic 'on' neurones by Wiersma and Yamaguchi (Wiersma and Yamaguchi, 1966; Wiersma and Yamaguchi, 1967), have their main dendritic tree in the medulla (Kirk et al., 1982) and respond to a light pulse with a phasotonic discharge that persists for the duration of the stimulus and is followed by an inhibitory 'off' response (Kirk et al., 1983; Pfeiffer and Glantz, 1989). They are additionally directionally selective to movement (Glantz et al., 1995). Similar responses to light have been recorded from sustaining fibres in crabs (Berón de Astrada et al., 2001; Berón de Astrada et al., 2009). It seems quite clear that the class of neurones we have been recording from that have their dendritic arborisations

in the medulla are sustaining fibres. The location of the dendritic tree (Fig. 7A) and the response to light pulses (Fig. 9A) are identical to those described above for such fibres. Additionally, our evidence that there are a number of these neurones, with receptive fields that together cover the whole visual field of the crab, is compatible with the 14 members of the sustaining fibre ensemble identified by Kirk et al. (Kirk et al., 1983).

We can be equally sure of the identity of the second group of optic flow sensitive neurones, those having their main dendritic arborisation in the lobula (or internal medulla to use the older nomenclature). From their responses to movement, it is clear that these neurones belong to the class of fibres called movement fibres by Wiersma et al. (Wiersma et al., 1982). In their early work, the Tomsic group called such fibres movement detector neurones (MDNs) (Berón de Astrada and Tomsic, 2002; Tomsic et al., 2003). The histological work of Sztarker et al. (Sztarker et al., 2005) demonstrated that MDNs were not a single morphological cell type; intracellular staining revealed two morphological subtypes, with dendrites restricted to a single stratum of the lobula (monostratified) or spread over two strata (bistratified). Each of these types can be further subdivided according to the size of their receptive fields, ~90 deg (type 1) or >180 deg (type 2). We thus end up with four morphological types (M1, M2, B1 and B2) according to Oliva et al. (Oliva et al., 2007), but renamed
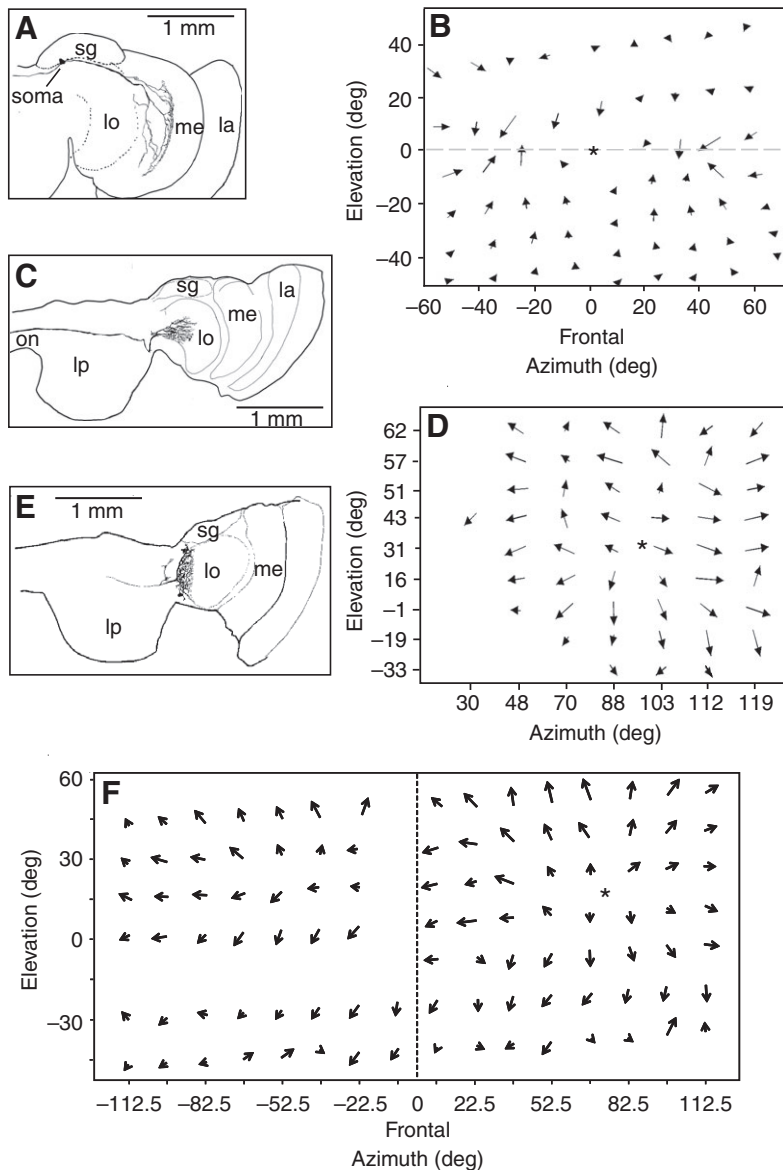
Fig. 7. Examples of Lucifer Yellow fills of identified wide-field visual *C. maenas* interneurones and their response maps. (A,B) Interneurone with its dendritic tree in the medulla of the right optic lobe (A) and its response map (B) showing a clear FOC (asterisk). (C,D) Interneurone with its dendritic field in the lobula of the right optic lobe (C) and its response map (D) showing a clear focus of expansion (FOE; asterisk). (E,F) Interneurone with its dendritic field covering the full width of the lobula of the right optic lobe (E) and its response map (F) showing a clear FOE (asterisk). la, lamina; lo, lobula; lp, lateral protocerebrum; me, medulla; on, optic nerve; sg, sinus gland.

monostratified and bistratified lobular giants 1 and 2 (MLG1, MLG2, BLG1 and BLG2) by Medan et al. (Medan et al., 2007). As well as their strong responses to small moving stimuli, they are characterised by brief excitatory responses (often just a single spike) to a light pulse at 'on' and 'off' (Medan et al., 2007). The response to movement, the location of the main dendritic arborisations in the lobula and the characteristic response to a light pulse (Fig. 9B) indicate that the lobular neurones we have been recording from are lobular giant neurones. Because we see dendrites restricted to a single plane (Fig. 7C,E), they are monostratified lobular giants. The majority of our recordings are from MLG1 neurones, as they have receptive fields covering approximately 90 deg of arc (Fig. 7D), with different neurones covering different parts of the visual field. Medan et al. identified 14 neurones in this category (Medan et al., 2007). On a few occasions, we recorded from neurones with much larger receptive fields (Fig. 7F), where the dendrites covered the full width of the lobula (Fig. 7E). These are clearly MLG2 neurones. Medan et al. suspect that there is only one neurone of this type (Medan et al., 2007), a conclusion with which we concur.

Are these populations of medulla and lobula neurones detectors of translational optic flow?

The methodology used here involved determining local motion sensitivity at 56 different points in the visual field. The resulting LPDs were then used to compile a response map representing the neurone's global motion sensitivity. The overriding advantage of this method over other stimuli that stimulate the whole receptive field at once is that the experimenter does not have to pre-judge the neurone's response pattern in order to provide an appropriate stimulus. The response pattern, whether it results from translational optic flow, rotational optic flow, looming or any other kind of motion sensitivity, makes itself apparent when compilation of the map of LPDs and LMSs is complete. This method has successfully been used to analyse neurones sensitive to optic flow in the blowfly's lobula plate (Krapp and Hengtstenberg, 1996; Krapp et al., 1998). These blowfly neurones also respond to global stimuli (Karmeier et al., 2003) and, when viewing panoramic virtual reality stimuli that take into account the saccadic head movements of the fly during flight, show responses to translational optic flow (Kern et al., 2005). On the basis of the performance of a simple model, the cyberfly,
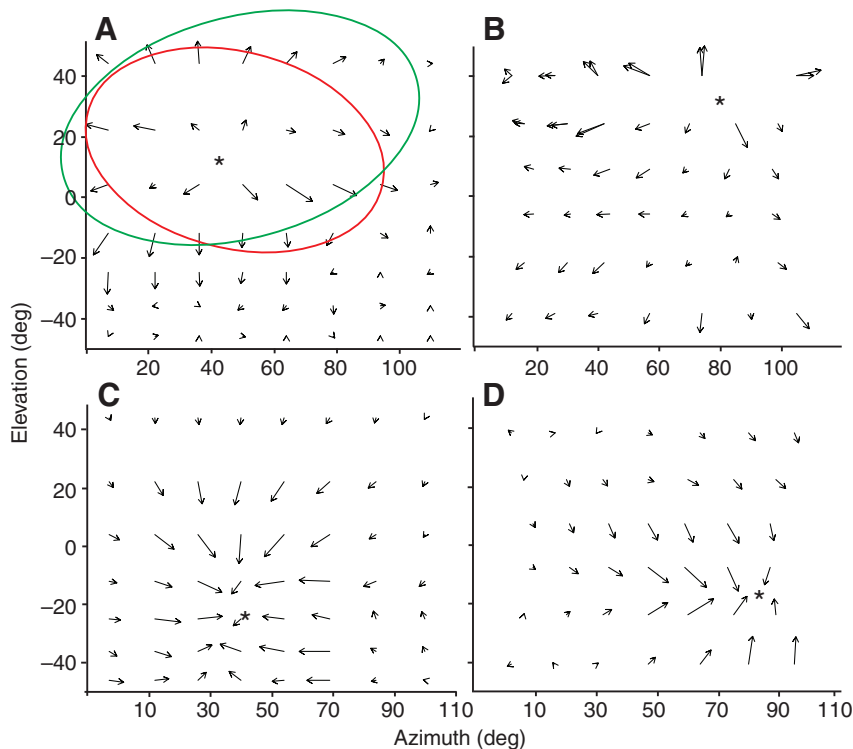
Fig. 8. Directionality of response maps of *C. maenas* lobula and medulla interneurones. (A,B) Response maps of two neurones recorded in the lobula of the right optic lobe of the same preparation. Both cells show motion sensitivity with an FOE (asterisk) ~40 deg to the right of frontal (A) and ~75 deg to the right of frontal (B). In both cases the neurones would be excited when the crab translated in the direction of their respective foci of expansion. The red oval in A shows the part of the receptive field where 'on' responses occurred in response to a flash of light, whereas the green oval shows the extent of 'off' responses to a flash of light. (C,D) Response maps of two neurones recorded in the medulla of the right optic lobe of a different preparation. Both cells show motion sensitivity with an FOC (asterisk) ~35 deg to the right of frontal (C) and ~80 deg to the right of frontal (D). These neurones would be excited when the crabs translated in a direction 180 deg away from their respective FOCs.

they may even play a role in obstacle avoidance (Lindemann et al., 2008).

The response maps we have obtained by the use of this analysis are just what you would expect of neurones responsive to optic flow (Fig. 10). Although we have not recorded from neurones sensitive to rotational optic flow (Fig. 10A), such neurones must exist as crabs show powerful optokinetic responses to rotation of a striped drum around the animal and to body turns (Barnes, 1990; Paul et al., 1998). The response maps of our populations of lobula and medulla neurones are, however, excellent matches to the patterns expected from neurones sensitive to translational optic flow. The maps of our population of lamina neurones are a good match to the pattern of vectors of an approaching scene (compare Fig. 8A,B with Fig. 10B), whereas the maps of medulla neurones are a similarly good match to the vector pattern of a receding scene (compare Fig. 8C,D with Fig. 10C). In each case there is a central pole, which is an FOE in the case of neurones sensitive to the approaching scene and an FOC in the case of neurones sensitive to the receding scene. Such poles would provide the crab with good visual information about its direction of travel.

LPDs are robust, as they are relatively insensitive to changes in the velocity of movement, changes in the method used to compile them (circular or linear motion) and changes in the shape of the stimulus object. Response maps are similarly robust (Fig. 6E). We are thus confident that the response maps of these populations of medulla and lobula neurones are truly representative of the neurones' global motion sensitivity. However, before we can be sure that they are indeed optic flow neurones, it is necessary to show that they respond to the appropriate global stimuli. Our preliminary experiments have failed to do this (data not shown). Perhaps this is not surprising. All the data analysis was carried out off-line, so that the properties of the neurone, its receptive field and the pole of the flow field only revealed themselves long after the experiment was over. Thus the likelihood of presenting the correct global stimulus

at the right location within the eye's field of view was relatively low.

An alternative possibility, for the lobula neurones only, is that they are neurones sensitive to looming and would trigger the crab's escape response, as has been shown in the crab *Chasmagnathus* (e.g. Sztarker and Tomsic, 2008). This possibility cannot be excluded, because looming neurones might be expected to produce response maps rather similar to those of translational optic flow. However, *C. maenas* has a lifestyle that is very different to that of *Chasmagnathus*. It remains hidden when the tide is low, and so would not be subject to the same predation risks as *Chasmagnathus*, a semi-terrestrial crab at constant risk from predation by seabirds (Bachmann and Martinez, 1999; Copello and Favero, 2001). Unlike *Chasmagnathus* lobula neurones, those of *C. maenas* do not show strong habituation, which is an important feature of neurones that elicit escape. Indeed, there is good evidence that, although different crab species (and, to a lesser extent, different decapods) do have homologous neurones, such neurones may become specialised for different functions according to the lifestyle of the species (Sztarker et al., 2005; Sztarker et al., 2009). It is also worth pointing out that a well-studied looming neurone in locusts, the lobula giant movement detector (LGMD) is not directionally selective (Krapp and Gabbiani, 2005); therefore, looming detection and optic flow processing are not necessarily linked.

Studies of the eye movements of freely moving crabs (Barnes, 1990; Paul et al., 1990; Paul et al., 1998) also lead us to expect that neurones sensitive to translational optic flow should exist, as crabs separate the rotational and translational components of their optic flow field as they move about their environment. They do this by using eye movements to compensate for the rotational component of their path by a variety of mechanisms (for details, see Barnes and Nalbach, 1993; Kern et al., 1993; Blanke et al., 1997). Because combinations of translation and rotation defy easy analysis, viewing only the translational component of optic flow makes available the
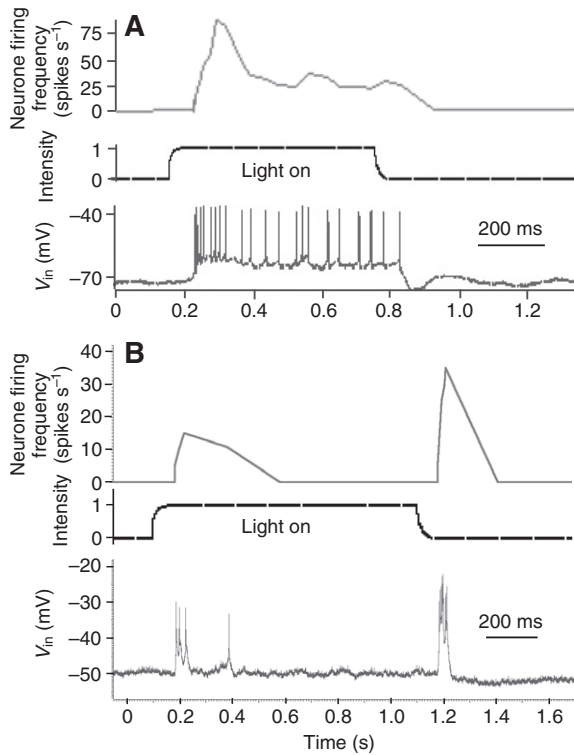
Fig. 9. Responses of *C. maenas* medulla and lobula interneurones to a flashing target (see Fig. 2C). (A) Phasotonic response of a medulla cell. (B) On/off response of a lobula cell. Intensity, light flash intensity; V_{in}, intracellular recorded membrane potential.

information it contains, including locomotor performance and the relative positions and distances of objects in the external world (Eckert and Zeil, 2001).

Possible function of these neurones

Given that crabs have 360 deg vision and predominantly walk sideways, having two classes of neurone – one responding to the approaching world and the other to the receding world – makes good sense. It doubles the amount of information that they receive and can use in a variety of ways. Indeed, as discussed in

mathematical terms by Dahmen et al. (Dahmen et al., 2001), the best estimates of egomotion are obtained with wide field neurones with opposite directions of view. As hypothesized by Gibson (Gibson, 1986), the information can be used to estimate velocity and distance travelled, to give distance information by motion parallax and assist in maintaining a heading. Which of these possibilities are likely to be of relevance to crabs? Recent research has demonstrated the importance of translational optic flow in estimating distance flown in flying insects (Srinivasan et al., 2000; Esch et al., 2001; Dacke and Srinivasan, 2008; Shafir and Barron, 2010), but there is little evidence that land arthropods estimate distance travelled using optic flow (Ronacher et al., 2000). Desert ants, whose homing behaviour has been intensively studied in recent years (e.g. Merkle and Wehner, 2010), use stride integration (summing of individual stride lengths) to estimate distance covered (Wittlinger et al., 2006; Wittlinger et al., 2007). Turning to crustaceans, fiddler crabs certainly use optomotor responses (generated by rotational optic flow) to compensate for deviations from their intended path (Layne et al., 1999) but, like ants, judge distance travelled by flexible stride integration (Layne et al., 2003a; Layne et al., 2003b; Walls and Layne, 2009a; Walls and Layne, 2009b). Homing, however, requires that the individual knows direction as well as distance, and recent evidence suggests that maintenance of the angle between the eye and the burrow (even when the actual burrow is no longer visible to the crab) is crucial to this (Layne, 2008) (J. E. Layne, W.J.P.B. and A. Dzwonczyk, unpublished observations). By maintaining this angle, the directional component of the home vector becomes a retinal location. If this angle is maintained during an excursion from the burrow, then keeping the retinal location of the home vector at the FOE during homing will ensure that home is reached. Retinal location is also key to both predator identification (Layne, 1998) and burrow defence (Hemmi and Zeil, 2003a; Hemmi and Zeil, 2003b). A possible role for this sophisticated system for the detection of translatory optic flow might thus be in the maintenance of a heading. Having the largest vectors near the pole of the flow field, as exhibited by the response maps illustrated in Fig. 8C,D, would help in this, though it must be remembered that the highest velocities of apparent movement lie at right angles to the direction of travel (at least for objects equidistant from the eye). Indeed, our results are the opposite of what has been found in the blowfly (Krapp et al., 1998), where FOEs are surrounded by small vectors. Could it be that the slower image motion (walking rather than flying) is compensated
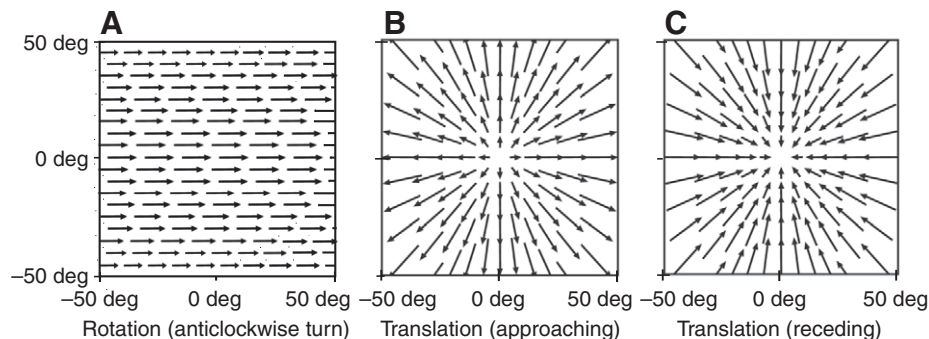

Fig. 10. Optic flow fields resulting from rotation (turning) and translation (straight-line movements) in an animal with 360 deg vision. (A) The animal rotates anticlockwise about its vertical axis. (B,C) The animal translates. Optic flow patterns seen by parts of the eye that are facing the direction of locomotion are shown in B, parts of the eye that are facing in the opposite direction are shown in C. In all cases, the arrows are velocity vectors representing the apparent movement of objects in the environment. In these simulations, all objects seen are equidistant from the eye. B and C are redrawn from van den Berg (van den Berg, 2000).

for by increased motion sensitivity? This strategy relies on a high signal to noise ratio, i.e. that the flow vectors are small but reliable. This is reasonable because compensatory eye movements effectively counteract the small rotational components inherent in the somewhat lurching gait of crabs (Barnes, 1990).

Directions for future work

These experiments were difficult to perform, and much work still is required. But, with the benefit of hindsight, we suspect that our *C. maenas* preparation, involving exsanguination and a significant amount of dissection, was not the best preparation to have chosen. The Tomsic group (Berón de Astrada and Tomsic, 2001) has clearly identified a much better method for carrying out such experiments, but whether it works as well for *C. maenas* as it does for *Chasmagnathus* remains to be investigated. An obvious gap in our knowledge is the way in which the neurones respond to global stimuli. However, if online data analysis were possible so that the response map was constructed while still having a microelectrode in the cell, it would be much easier to choose an appropriate global stimulus. A second knowledge gap is the extent to which our two populations of neurones consist of arrays of cells with poles at different azimuth angles. Sztarker et al. have now done the anatomy (Sztarker et al., 2005; Sztarker et al., 2009), so future work can build up a picture of the arrays of cells specialized for sensing translational optic flow and the extent to which they interact with each other, perhaps by electrical synapses, as do neurones with similar properties in flies (Haag and Borst, 2005). Finally, we have yet to determine the properties of neurones in the lobula plate of crabs – which may be homologous to that of insects (Strausfeld, 2005) – the area where insect optic flow neurones are found (Krapp et al., 1998).

ACKNOWLEDGEMENTS

REFERENCES

Bachmann, S. and Martinez, M. M. (1999). Feeding tactics of the American oystercatcher (*Haematopus palliates*) on Mar Chiquita coastal lagoon, Argentina. *Ornitol. Neotrop.* **10**, 81-84.

Barnes, W. J. P. (1990). Sensory basis and functional role of eye movements elicited during locomotion in the land crab, *Cardisoma guanhumi. J. Exp. Biol.* **154**, 99-119.

Barnes, W. J. P. and Horridge, G. A. (1969). Interaction of the movement of the two eyecups in the crab, *Carcinus. J. Exp. Biol.* **50**, 651-671.

Barnes, W. J. P. and Nalbach, H.-O. (1993). Eye movements in freely moving crabs: their sensory basis and possible role in flow-field analysis. *Comp. Biochem. Physiol.* **104A**, 675-693.

Barnes, W. J. P., Horseman, B. G. and Macauley, M. W. S. (2001). The detection and analysis of optic flow by crabs: from eye movements to electrophysiology. In *The Crustacean Nervous System* (ed. K. Wiese), pp. 468-485. Berlin, Heidelberg and New York: Springer Verlag.

Barnes, W. J. P., Johnson, A. P., Horseman, G. B. and Macauley, M. W. S. (2002). Computer-aided studies of vision in crabs. *Mar. Freshw. Behav. Physiol.* **35**, 37-56.

Batschelet, E. (1981). *Circular Statistics in Biology.* London: Academic Press.

Berón de Astrada, M. and Tomsic, D. (2002). Physiology and morphology of visual movement detector neurons in a crab (Decapoda: Brachyura). *J. Comp. Physiol. A* **188**, 539-551.

Berón de Astrada, M., Sztarker, J. and Tomsic, D. (2001). Visual interneurons of the crab *Chasmagnathus* studied by intracellular recordings in vivo. *J. Comp. Physiol.* **187**, 37-44.

Berón de Astrada, M., Tuthill, J. C. and Tomsic, D. (2009). Physiology and morphology of sustaining and dimming neurons of the crab *Chasmagnathus granulatus* (Brachyura: Grapsidae). *J. Comp. Physiol. A* **195**, 7919-7798.

Blanke, H., Nalbach, H.-O. and Varjú, D. (1997). Whole-field integration, not detailed analysis, is used by the crab optokinetic system to separate rotation and translation in optic flow. *J. Comp. Physiol. A* **181**, 383-392.

Bremmer, F., Duhamel, J. R., Hamed, S. B. and Graf, W. (2002). Heading encoding in the macaque ventral intraparietal area (VIP). *Eur. J. Neurosci.* **16**, 1554-1568.

Bush, B. M. H. and Roberts, A. (1971). Coxal muscle receptors in the crab: the receptor potentials of S and T fibers in response to ramp stretches. *J. Exp. Biol.* **55**, 813-832.

Collett, T. S. and Land, M. F. (1975). Visual control of flight behaviour in the hoverfly, *Syritta pipiens.* L. *J. Comp. Physiol. A* **99**, 1-66.

Copello, S. and Favero, M. (2001). Foraging ecology of Olrog's gull *Larus atlanticus* in Mar Chiquita lagoon (Buenos Aires, Argentina): are there age-related differences? *Bird Conserv. Int.* **11**, 175-188.

Dacke, M. and Srinivasan, M. V. (2008). Two odometers in honeybees? *J. Exp. Biol.* **211**, 3281-3286.

Dahmen, H.-J., Franza, M. O. and Krapp, H. G. (2001). Extracting egomotion from optic flow: limits of accuracy and neural matched filters. In *Motion Vision – Computational, Neural and Ecological Constraints* (ed. J. M. Zanker and J. Zeil), pp. 143-168. Berlin, Heidelberg and New York: Springer Verlag.

David, C. T. (1982). Compensation for height in the control of groundspeed by *Drosophila* in a new 'barber's pole' wind tunnel. *J. Comp. Physiol.* **147**, 485-493.

Eckert, M. P. and Zeil, J. (2001). Towards an ecology of motion vision. In *Motion Vision – Computational, Neural and Ecological Constraints* (ed. J. M. Zanker and J. Zeil), pp. 333-369. Berlin, Heidelberg and New York: Springer Verlag.

Esch, H. E., Zhang, S., Srinivasan, M. V. and Tautz, J. (2001). Honeybee dances communicate distances measured by optic flow. *Nature* **411**, 581.

Farina, W. M., Varjú, D. and Zhou, Y. (1994). The regulation of distance to dummy flowers during hovering flight in the hawk moth. *Macroglossum stellatarum. J. Comp. Physiol.* **174**, 239-247.

Gibson, J. J. (1950). *The Perception of the Visual World.* Boston, MA: Houghton Mifflin.

Gibson, J. J. (1966). *The Senses Considered as Perceptual Systems.* Boston, MA: Houghton Mifflin.

Gibson, J. J. (1986). *The Ecological Approach to Visual Perception.* Boston, MA: Houghton Mifflin.

Glantz, R. M. and Bartels, A. (1994). The spatiotemporal transfer function of crayfish lamina monopolar neurons. *J. Neurophysiol.* **71**, 2168-2182.

Glantz, R. M. and Miller, C. S. (2001). Signal processing in the crayfish optic lobe: contrast, motion and polarization vision. In *The Crustacean Nervous System* (ed. K. Wiese), pp. 486-498. Berlin, Heidelberg and New York: Springer Verlag.

Glantz, R. M., Wyatt, C. and Mahncke, H. (1995). Directionally selective motion detection in the sustaining fibers of the crayfish optic nerve – linear and nonlinear mechanisms. *J. Neurophysiol.* **74**, 142-152.

Götz, K. G. (1975). The optomotor equilibrium of the *Drosophila* navigation system. *J. Comp. Physiol. A* **99**, 187-210.

Green, W. E., Oh, P. Y. and Barrows, G. (2004). Flying insect inspired vision for autonomous aerial robot maneuvers in near-earth environments. *IEEE Int. Conf. Robot. Autom.* **3**, 2347-2352.

Haag, J. and Borst, A. (2004). Neural mechanism underlying complex receptive field properties of motion-sensitive interneurons. *Nat. Neurosci.* **7**, 628-634.

Haag, J. and Borst, A. (2005). Dye-coupling visualizes networks of large-field motion-sensitive neurons in the fly. *J. Comp. Physiol. A* **191**, 445-454.

Hassenstein, B. and Reichardt, W. (1956). Systemtheoretische Analyse der Zeit-, Reihenfolgen- und Vorzeichenauswertung bei der Bewegungsperzeption des Rüsselkäfers *Chlorophanus. Z. Naturforsch.* **11**, 513-524.

Hausen, K. (1982a). Motion sensitive interneurons in the optomotor system of the fly. I. The horizontal cells: structure and signals. *Biol. Cybern.* **45**, 143-156.

Hausen, K. (1982b). Motion sensitive interneurons in the optomotor system of the fly. II. The horizontal cells: receptive field organization and response characteristics. *Biol. Cybern.* **46**, 67-79.

Hausen, K. (1984). The lobula complex of the fly: structure, function and significance in visual behaviour. In *Photoreception and Vision in Invertebrates* (ed. M. A. Ali), pp. 523-599. New York: Plenum Press.

Hausen, K. and Egelhaaf, M. (1989). Neural mechanisms of visual course control in insects. In *Facets of Vision* (ed. G. G. Stavenga and R. C. Hardie), pp. 391-424. Berlin, Heidelberg and New York: Springer Verlag.

Hemmi, J. M. and Zeil, J. (2003a). Burrow surveillance in fiddler crabs. I. Description of behaviour. *J. Exp. Biol.* **206**, 3935-3950.

Hemmi, J. M. and Zeil, J. (2003b). Burrow surveillance in fiddler crabs. II. The sensory cues. *J. Exp. Biol.* **206**, 3951-3961.

Holmqvist, M. H. and Srinivasan, M. V. (1991). A visually evoked escape response of the housefly. *J. Comp. Physiol. A* **169**, 451-459.

Horridge, G. A. (1966). The optomotor response of the crab, *Carcinus.* In *Information Processing in Sight Sensory Systems* (ed. P. W. Nye), pp. 57-74. Pasadena, CA: California Institute of Technology.

Horridge, G. A. and Sandeman, D. C. (1964). Nervous control of optokinetic responses in the crab *Carcinus. Proc. R. Soc. Lond. B Biol. Sci.* **161**, 216-246.

Hyslop, A., Krapp, H. G. and Humbert, J. S. (2010). Control theoretic interpretation of directional motion preferences in optic flow processing interneurons. *Biol. Cybern.* **103**, 353-364.

Johnson, A. P., Horseman, B. G., Macauley, M. W. S. and Barnes, W. J. P. (2002). PC-based visual stimuli for behavioural and electrophysiological studies of optic flow field detection. *J. Neurosci. Methods* **114**, 51-61.

Karmeier, K., Krapp, H. G. and Egelhaaf, M. (2003). Robustness of the tuning of fly visual interneurons to rotatory optic flow. *J. Neurophysiol.* **90**, 1626-1634.

Kern, R., Nalbach, H.-O. and Varjú, D. (1993). Interactions of local movement detectors enhance the detection of rotation. Optokinetic experiments with the rock crab, *Pachygrapsus marmoratus. Vis. Neurosci.* **10**, 643-646.

Kern, R., van Hateren, J. H., Michaelis, C., Lindemann, J. P. and Egelhaaf, M. (2005). Function of a fly motion-sensitive neuron matches eye movements during free flight. *PloS Biol.* **3**, 1130-1138.

Kirk, M. D., Waldrop, B. and Glantz, R. M. (1982). The crayfish sustaining fibers. I. Morphological representation of visual receptive fields in the second optic neuropil. *J. Comp. Physiol.* **146**, 419-425.

Kirk, M. D., Waldrop, B. and Glantz, R. M. (1983). The crayfish sustaining fibers. II. Response to illumination, membrane properties and adaptation. *J. Comp. Physiol.* **150**, 175-179.

Koenderink, J. J. and van Doorn, A. (1987). Facts on optic flow. *Biol. Cybern.* **56**, 247-254.

Krapp, H. G. (2000). Neuronal matched filters for optic flow processing in flying insects. In *Neuronal Processing of Optic Flow* (ed. M. Lappe), pp. 93-120. San Diego, CA: Academic Press.

Krapp, H. G. and Gabbiani, F. (2005). Spatial distribution of inputs and local receptive field properties of a wide-field, looming sensitive neuron. *J. Neurophysiol.* **93**, 2240-2253.

Krapp, H. G. and Hengstenberg, R. (1996). Estimation of self-motion by optic flow processing in single visual interneurons. *Nature* **384**, 463-466.

Krapp, H. G. and Hengstenberg, R. (1997). A fast stimulus procedure to determine local receptive field properties of motion-sensitive visual interneurons. *Vis. Res.* **37**, 225-234.

Krapp, H. G., Hengstenberg, B. and Hengstenberg, R. (1998). Dendritic structure and receptive-field organization of optic flow processing interneurons in the fly. *J. Neurophysiol.* **79**, 1902-1917.

Land, M. F. (1981). Optics and vision in invertebrates. In *Handbook of Sensory Physiology,* Vol. VII/6B (ed. H. Autrum), pp. 471-592. Berlin: Springer Verlag.

Land, M. F. (1999). Motion and vision: why animals move their eyes. *J. Comp. Physiol.* **185**, 341-352.

Land, M. F. and Nilsson, D.-E. (2002). *Animal Eyes.* Oxford: Oxford University Press.

Layne, J. E. (1998). Retinal location is the key to identifying predators in fiddler crabs (*Uca pugilator*). *J. Exp. Biol.* **201**, 2253-2261.

Layne, J. E. (2008). Visually mediated stabilizing reflexes dictate the direction of the path-integrated home vector. *2nd Int. Conf. Invertebr. Vis. Sweden*, p. 86.

Layne, J. E., Wicklein, M., Dodge, F. A. and Barlow, R. B. (1997). Prediction of maximal allowable retinal slip speed in the fiddler crab, *Uca pugilator. Biol. Bull.* **193**, 202-203.

Layne, J. E., Barnes, W. J. P. and Duncan, L. M. J. (1999). Homing in fiddler crabs: kinaesthetic path integration and the optomotor response. *In Göttingen Neurobiology Report 1999* (ed. N. Elsner and U. Eysel). 417 pp. Stuttgart and New York: Georg Thieme Verlag.

Layne, J. E., Barnes, W. J. P. and Duncan, L. M. J. (2003a). Mechanisms of homing in the fiddler crab *Uca rapax.* I. Spatial and temporal characteristics of a system of small-scale navigation. *J. Exp. Biol.* **206**, 4413-4423.

Layne, J. E., Barnes, W. J. P. and Duncan, L. M. J. (2003b). Mechanisms of homing in the fiddler crab *Uca rapax.* II. Information sources and frame of reference for a path integration system. *J. Exp. Biol.* **206**, 4425-4442.

Lindemann, J. P., Weiss, H., Möller, R. and Egelhaaf, M. (2008). Saccadic flight strategy facilitates collision avoidance: closed-loop performance of a cyberfly. *Biol. Cybern.* **98**, 213-227.

Medan, V., Oliva, D. and Tomsic, D. (2007). Characterization of lobula giant neurons responsive to visual stimuli that elicit escape behaviors in the crab *Chasmagnathus. J. Neurophysiol.* **98**, 2414-2428.

Merkle, T. and Wehner, R. (2010). Desert ants use foraging distance to adapt the nest search to the uncertainty of the path integrator. *Behav. Ecol.* **21**, 349-355.

Nilsson, D.-E. (1988). A new type of imaging optics in compound eyes. *Nature* **332**, 76-78.

Oliva, D., Medan, V. and Tomsic, D. (2007). Escape behavior and neuronal responses to looming stimuli in the crab *Chasmagnathus granulatus* (Decapoda: Grapsidae). *J. Exp. Biol.* **210**, 865-880.

Paolini, M., Distler, C., Bremmer, F., Lappe, M. and Hoffmann, K.-P. (2000). Responses to continuously changing optic flow in area MST. *J. Neurophysiol.* **84**, 730-743.

Paul, H., Nalbach, H.-O. and Varjú, D. (1990). Eye movements in the rock crab *Pachygrapsus marmoratus* walking along straight and curved paths. *J. Exp. Biol.* **154**, 81-97.

Paul, H., Barnes, W. J. P. and Varjú, D. (1998). Roles of eyes, leg proprioceptors and statocysts in the compensatory eye movements of freely walking land crabs (*Cardisoma guanhumi*). *J. Exp. Biol.* **201**, 3395-3409.

Pearson, J. (1908). Cancer. In *Liverpool Marine Biological Committee Memoirs on Typical Marine Plants and Animals, No. XVI* (ed. W. A. Herdman), pp. 1-209. London: Williams and Norgate.

Pfeiffer, C. and Glantz, R. M. (1989). Cholinergic synapses and the organization of contrast detection in the crayfish optic lobe. *J. Neurosci.* **9**, 1872-1882.

Ronacher, B., Gallizzi, K., Wohlgemuth, S. and Wehner, R. (2000). Lateral optic flow does not influence distance estimation in the desert ant *Cataglyphis fortis. J. Exp. Biol.* **203**, 1113-1121.

Saito, H., Yukie, M., Tanaka, K., Hikosaka, K., Fukada, Y. and Iwai, E. (1986). Integration of direction signals of image motion in the superior temporal sulcus of the macaque monkey. *J. Neurosci.* **6**, 145-157.

Shafir, S. and Barron, A. B. (2010). Optic flow informs distance but not profitability for honeybees. *Proc. R. Soc. Lond. B Biol. Sci.* **277**, 1241-1245.

Simpson, J. I., Graf, W. and Leonard, C. (1981). The coordinate system of visual climbing fibres to the flocculus. In *Progress in Oculomotor Research* (ed. A. F. Fuchs and W. Becker) pp. 475-484. Amsterdam: Elsevier.

Srinivasan, M. V., Lehrer, M., Kirchner, W. H. and Zhang, S. W. (1991). Range perception through apparent image speed in freely flying honey bees. *Vis. Neurosci.* **6**, 519-535.

Srinivasan, M. V., Chahl, J. S., Weber, K., Venkatesh, S., Nagle, M. G. and Zhang, S. W. (1999). Robot navigation inspired by principles of insect vision. *Robot. Auton. Syst.* **26**, 203-216.

Srinivasan, M. V., Zhang, S. W., Altwein, M. and Tautz, J. (2000). Honeybee navigation: nature and calibration of the 'odometer'. *Science* **287**, 851-853.

Stewart, W. W. (1978). Functional connections between cells as revealed by dye-coupling with a highly fluorescent naphthalimide tracer. *Cell* **14**, 741-759.

Strausfeld, N. (2005). The evolution of crustacean and insect optic lobes and the origin of chiasmata. *Arthropod. Struct. Dev.* **34**, 235-256.

Sun, H. and Frost, B. J. (1998). Computation of different optical variables of looming objects in pigeon nucleus rotundus neurons. *Nat. Neurosci.* **1**, 296-303.

Sztarker, J. and Tomsic, D. (2008). Neuronal correlates of the visually elicited escape response of the crab *Chasmagnathus* upon seasonal variations, stimuli changes and perceptual alterations. *J. Comp. Physiol. A* **194**, 587-596.

Sztarker, J., Strausfeld, N. J. and Tomsic, D. (2005). Organization of optic lobes that support motion detection in a semiterrestrial crab, *J. Comp. Neurol.* **493**, 396-411.

Sztarker, J., Strausfeld, N. J., Andrew, D. and Tomsic, D. (2009). Neural organization of first optic neuropils in the littoral crab *Hemigrapsus oregonensis* and the semiterrestrial species *Chasmagnathus granulatus. J. Comp. Neurol.* **513**, 129-150.

Tammero, L. F. and Dickinson, M. H. (2002). Collision-avoidance and landing responses are mediated by separate pathways in the fruit fly, *Drosophila melanogaster. J. Exp. Biol.* **205**, 2785-2798.

Tanaka, K. and Saito, H. (1989). Analysis of motion of the visual field by direction, expansion/contraction, and rotation cells clustered in the dorsal part of the medial superior temporal area of the macaque monkey. *J. Neurophysiol.* **62**, 626-641.

Taylor, G. K. and Krapp, H. G. (2007). Sensory systems and flight stability: what do insects measure and why? *Adv. Insect Physiol.* **34**, 231-316.

Tomsic, D., Béron de Astrada, M. and Sztarker, J. (2003). Identification of individual neurons reflecting short- and long-term visual memory in an arthropod. *J. Neurosci.* **23**, 8539-8546.

van den Berg, A. V. (2000). Human ego-motion perception. In *Neuronal Processing of Optic Flow* (ed. M. Lappe), *Int. Rev. Neurobiol.*, vol. 44, pp. 3-25. London: Academic Press.

Wagner, H. (1982). Flow-field variables trigger landing in flies. *Nature* **297**, 147-148.

Walls, M. L. and Layne, J. E. (2009a). Direct evidence for distance measurement via flexible stride integration in the fiddler crab. *Curr. Biol.* **19**, 1-5.

Walls, M. L. and Layne, J. E. (2009b). Fiddler crabs accurately measure two-dimensional distance over three-dimensional terrain. *J. Exp. Biol.* **212**, 3236-3240.

Wang, Y. C. and Frost, B. J. (1992). Time to collision is signaled by neurons in the nucleus rotundus of pigeons. *Nature* **356**, 236-238.

Waterman, T. H., Wiersma, C. A. G. and Bush, B. M. H. (1964). Afferent visual responses in the optic nerve of the crab *Podophthalmus. J. Cell. Comp. Physiol.* **63**, 135-155.

Wicklein, M. and Strausfeld, N. J. (2000). Organization and significance of neurons that detect change of visual depth in the hawk moth *Manduca sexta. J. Comp. Neurol.* **424**, 356-376.

Wiersma, C. A. G. (1966). Integration in the visual pathway of Crustacea. *Symp. Soc. Exp. Biol.* **20**, 151-177.

Wiersma, C. A. G. and Yamaguchi, T. (1966). The neural components of the optic nerve of the crayfish as studied by single unit analysis. *J. Comp. Neurol.* **128**, 333-358.

Wiersma, C. A. G. and Yamaguchi, T. (1967). Integration of visual stimuli by the crayfish central nervous system. *J. Exp. Biol.* **47**, 409-431.

Wiersma, C. A. G., Roach, J. L. M. and Glantz, R. M. (1982). Neural integration in the optic system. In *The Biology of Crustacea, Vol. 4, Neural Integration and Behaviour* (ed. D. C. Sandeman and H. L. Atwood), pp. 1-31. New York: Academic Press.

Wittlinger, M., Wehner, R. and Wolf, H. (2006). The ant odometer: stepping on stilts and stumps. *Science* **312**, 1965-1967.

Wittlinger, M., Wehner, R. and Wolf, H. (2007). The ant odometer: a stride indicator that accounts for stride length and walking speed. *J. Exp. Biol.* **210**, 198-207.

Wylie, D. R. W. and Frost, B. J. (1993). Responses of neurons in the nucleus of the basal optic root to translational and rotational flowfields. *J. Neurophysiol.* **81**, 267-276.

York, B. and Wiersma, C. A. G. (1975). Visual processing in the rock lobster (crustacea). *Prog. Neurobiol.* **5**, 127-166.

Zeil, J. and Zanker, J. M. (1997). A glimpse into crabworld. *Vis. Res.* **37**, 3417-3426.

Zeil, J., Nalbach, G. and Nalbach, H.-O. (1986). Eyes, eye stalks and the visual world of semi-terrestrial crabs. *J. Comp. Physiol.* **159**, 801-811.

Zeil, J., Nalbach, G. and Nalbach, H.-O. (1989). Spatial vision in a flat world: optical and neural adaptations in arthropods. In *Neurobiology of Sensory Systems* (ed. R. N. Singh and N. J. Strausfeld), pp. 123-137. London and New York: Plenum.